OCCAM

OXFORD CENTRE FOR COLLABORATIVE APPLIED MATHEMATICS

Air-cushioning in impact problems

by

M. R. Moore
J. R. Ockendon
J. M. Oliver

OCCAM Preprint Number 12/104

IMA Journal of Applied Mathematics (2012) 1−21
doi: 10.1093/imamat/Under review

Air-cushioning in impact problems

M. R. MOORE, J. R. OCKENDON AND J. M. OLIVER
Mathematical Institute, University of Oxford,
24-29 St. Giles', Oxford, OX1 3LB, UK.

[Submitted November 2012]

This paper concerns the displacement potential formulation to study the post-impact influence of an air-cushioning layer on the two-dimensional impact of a liquid half-space by a rigid body. The liquid and air are both ideal and incompressible and attention is focussed on cases when the density ratio between the air and liquid is small. In particular, the correction to classical Wagner theory is analysed in detail for the impact of circular cylinders and wedges.

Keywords: Impact problems, air-cushioning, water entry.

1. Introduction

This paper describes some models for air-cushioning when a two-dimensional rigid impactor penetrates an incompressible liquid half-space. The impact is violent enough that the air can be modelled as an inviscid fluid, and the timescale is long enough that air compressibility can be neglected. Thus our theory complements that of Purvis & Smith (2004), who considered a lubrication theory model for the cushioning layer, building on the work of Smith *et al.* (2003), who described the influence of a lubricating air layer prior to impact. Similar pre-impact analysis is performed by Hicks & Purvis (2010) and Duchemin & Josserand (2011) who considered axisymmetric and three-dimensional geometries, Vanden-Broeck & Smith (2008) who included surface tension and Mandre & Brenner (2012) who discussed a compressible air model. These studies are supported by experimental investigations by, among others, Xu *et al.* (2005), Driscoll & Nagel (2011), de Ruiter *et al.* (2012) and Kolinski *et al.* (2012).

The basic cushioning model is set up and nondimensionalised in Section 2 to reveal the key parameters as the deadrise angle, ε, between the impactor and the half-space and the air-liquid density ratio, ρ. When both $\varepsilon \ll 1$ and $\lambda = \rho/\varepsilon \lesssim 1$, the lowest-order asymptotic structure is that of the well-known Wagner theory, as described by Wagner (1932), Armand & Cointe (1987) and Howison *et al.* (1991), except that the pressure is no longer constant at the air-liquid interface. However, it is only when $\lambda \ll 1$ that explicit expressions can be found for the liquid and gas flows, and in particular for the location of the so-called 'turnover regions' that form the roots of the splash jets. In this latter limit, the air flow responds to the liquid dynamics everywhere in the cushioning region.

As in Moore *et al.* (2012), even when $\lambda = O(1)$, the coupled air-liquid model is most conveniently written in terms of the displacement potential in the liquid, as first used for impact problems by Korobkin (1988).

In Section 3, we restrict our considerations to impacts where λ is small. In particular, we look at parabolic impactors, which are susceptible to a fairly complete analysis when both λ and ε are small. We also show how the cushioning model can be matched to the global air motion that is generated when a circular cylinder impacts a liquid half-space.

In Section 4, we consider the famous case of symmetric wedge impact, where the geometric simplicity allows a global similarity solution to exist in the air and in the liquid. Unfortunately, the geometry

is such that the relevant far-field conditions are unclear unless λ is small, but we are able to make some conjectures about this.

2. The model

We consider the effects of a cushioning air layer when a shallow, rigid impactor enters a liquid half-space that lies in $y^* < 0$; here and hereafter, an asterisk indicates a dimensional variable. At time $t^* = 0$, the impactor is assumed to be touching the liquid half-space, with air filling the region not occupied by the body or the liquid. We impulsively move the body so that at times $t^* > 0$ its position is given by

$$\frac{y^*}{L} = f\left(\frac{\varepsilon x^*}{L}\right) - \frac{V_0}{L}t^*,$$

where L is a characteristic penetration depth, $V_0 > 0$ is the impact speed and (x^*, y^*) are Cartesian coordinates centred at the initial touch point. The function f, which will be taken to be even for simplicity, is such that $f(0) = 0$ and f increases as $|x^*|$ increases. The parameter ε is a measure of the shallowness of the impactor and is called the deadrise angle. In much of this paper we will consider profiles in which the deadrise angle is small.

As in Wagner theory, we assume that the liquid is incompressible, inviscid and initially quiescent, with density ρ_l. For times $t^* > 0$, the impactor penetrates the liquid, causing the free surface to be violently disturbed. Two splash jets are assumed to form along the sides of the impactor. We denote the free surface by $y^* = h^*(x^*, t^*)$: as in the classical theory, this is multivalued for $t^* > 0$ and we denote the two turnover points where $\partial h^*/\partial x^*$ is unbounded by $x^* = \pm d^*(t^*)$. For the sake of analysis in the air region, it is important to consider the components of the free surface *above* the turnover point (i.e. the jet), denoted by $y^* = f(\varepsilon x^*/L) - (V_0/L)t^* - h^*_+$, and the free surface *below* the turnover point (i.e. bounding the bulk of the liquid), denoted by $y^* = h^*_-$, separately. The wetted extent of the impactor is defined as that between the two jet tips, which we denote by $x^* = \pm c^*(t^*)$.

We assume that the air is incompressible and inviscid with density ρ_a. Throughout, we will neglect the influence of gravity and surface tension. For a discussion of whether these assumptions are reasonable, the reader is directed to Howison *et al.* (2005). The problem configurations for $t^* = 0$ and $t^* > 0$ are illustrated in Figure 1.

Henceforth, we shall use lower-case letters to denote variables in the liquid and upper-case letters to denote variables in the air. In both the liquid and the air, the flow is irrotational with potentials ϕ^*, Φ^* respectively satisfying

$$\nabla^2\phi^* = 0 \quad \text{in the liquid,} \quad \nabla^2\Phi^* = 0 \quad \text{in the air,} \tag{2.1}$$

where ∇ is the gradient operator.

We must demand that there is no flow through the impactor in both regions, so that we require

$$\frac{\partial\phi^*}{\partial n*} = v_{n,b} \quad \text{on} \quad \frac{y^*}{L} = f\left(\frac{\varepsilon x^*}{L}\right) - \frac{V_0}{L}t^*, |x^*| < c^*(t^*), \tag{2.2}$$

$$\frac{\partial\Phi^*}{\partial n^*} = v_{n,b} \quad \text{on} \quad \frac{y^*}{L} = f\left(\frac{\varepsilon x^*}{L}\right) - \frac{V_0}{L}t^*, |x^*| > c^*(t^*), \tag{2.3}$$

where $\partial/\partial n^*$ represents the normal derivative to the free surface and $v_{n,b}$ is the outward normal speed of the impactor.

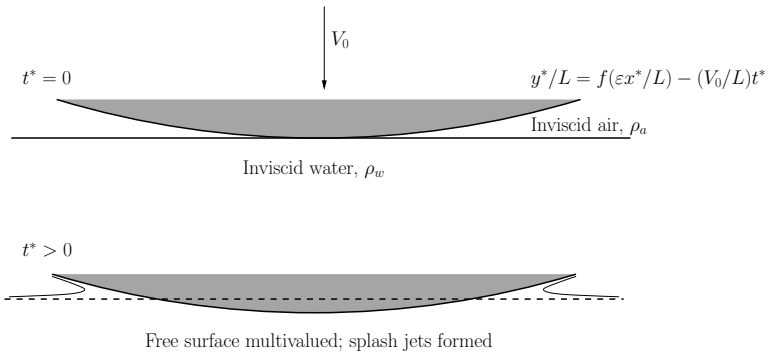

FIG. 1. A symmetric, rigid-body impact with the inclusion of an inviscid air-cushioning layer.

On the multivalued free surface, the kinematic conditions in the air and the liquid are given by

$$\frac{\partial \phi^*}{\partial n^*} = \frac{\partial \Phi^*}{\partial n^*} = v_{n,h} \quad \text{on} \quad y^* = h^*(x^*,t^*),\, |x^*| > d^*(t^*), \tag{2.4}$$

where $v_{n,h}$ is the outward normal speed of the boundary. Moreover, in the absence of viscosity and surface tension, the dynamic boundary condition is given by

$$p^* = P^* \quad \text{on} \quad y^* = h^*(x^*,t^*),\, |x^*| > d^*(t^*), \tag{2.5}$$

where $p^*(x^*,y^*,t^*)$, $P^*(x^*,y^*,t^*)$ are the pressures in the liquid and air respectively, which are related to the velocity potentials via

$$\frac{\partial \phi^*}{\partial t^*} + \frac{p^*}{\rho_l} + \frac{1}{2}|\nabla \phi^*|^2 = 0, \tag{2.6}$$

$$\frac{\partial \Phi^*}{\partial t^*} + \frac{P^*}{\rho_a} + \frac{1}{2}|\nabla \Phi^*|^2 = 0. \tag{2.7}$$

Initially, we assume that

$$\phi^*(x^*,y^*,0) = 0, \quad \Phi^*(x^*,y^*,0) = 0, \quad h^*(x^*,0) = 0, \quad c^*(0) = 0, \quad d^*(0) = 0. \tag{2.8}$$

With hindsight, in the far-field, we assume that the velocity potential in the liquid is no more singular than a point source and therefore that in order for global conservation of mass to be satisfied in the leading-order problem, we require the free surface displacement from its initial position to be integrable. However, the precise far-field conditions depend on the shape of the impactor and these will be discussed in the next section.

2.1 *Nondimensionalisation*

We nondimensionalise distances using a typical penetration depth L , velocities using the impact speed V_0, time with L/V_0, velocity potential with LV_0 and pressure with $\rho_i V_0^2$, where i is a, l in the air and liquid

respectively. Nondimensional variables are indicated with a prime. The dimensionless body profile is given by

$$y' = f(\varepsilon x') - t'.$$

Hence, the equations of motion are given by:

$$\nabla^2 \phi' = 0 \quad \text{in the liquid,} \quad \nabla^2 \Phi' = 0 \quad \text{in the air,} \tag{2.9}$$

where the kinematic conditions on the body are

$$\frac{\partial \phi'}{\partial y'} = -1 + \varepsilon f'(\varepsilon x') \frac{\partial \phi'}{\partial x'} \quad \text{on} \quad y' = f(\varepsilon x') - t', \, |x'| < c'(t'), \tag{2.10}$$

$$\frac{\partial \Phi'}{\partial y'} = -1 + \varepsilon f'(\varepsilon x') \frac{\partial \Phi'}{\partial x'} \quad \text{on} \quad y' = f(\varepsilon x') - t', \, |x'| > c'(t'), \tag{2.11}$$

where $f'(\cdot)$ indicates differentiation with respect to argument. The kinematic conditions on the free surface are given by

$$\frac{\partial \phi'}{\partial n'} = \frac{\partial \Phi'}{\partial n'} = v_{n,h} \quad \text{on} \quad y' = h'(x',t'), \, |x'| > d'(t'), \tag{2.12}$$

while the dynamic boundary condition is

$$p' = \rho P' \quad \text{on} \quad y' = h'(x',t'), \, |x'| > d'(t'), \tag{2.13}$$

where $\rho = \rho_a / \rho_l$ is the density ratio and

$$\frac{\partial \phi'}{\partial t'} + p' + \frac{1}{2} \left| \nabla \phi' \right|^2 = 0, \tag{2.14}$$

$$\frac{\partial \Phi'}{\partial t'} + P' + \frac{1}{2} \left| \nabla \Phi' \right|^2 = 0. \tag{2.15}$$

The initial conditions remain

$$\phi'(x',y',0) = 0, \quad \Phi'(x',y',0) = 0, \quad h'(x',0) = 0, \quad c'(0) = 0, \quad d'(0) = 0. \tag{2.16}$$

In the far-field, we make the apparently conservative assumption that the liquid and air flows are no stronger than sources with unknown strengths Q_1, Q_2 respectively, so that

$$\phi' = \frac{Q_1(t')}{\pi} \log r' + o(1) \quad \text{as} \quad r' = (x'^2 + y'^2)^{1/2} \to \infty, \tag{2.17}$$

$$\Phi' = \frac{Q_2(t')}{\pi} \log r' + o(1) \quad \text{as} \quad r' = (x'^2 + y'^2)^{1/2} \to \infty, \tag{2.18}$$

$$\tag{2.19}$$

where we expect the $o(1)$ terms to represent dipoles. Furthermore,

$$h'_- = o\left(\frac{1}{x'}\right) \quad \text{as} \quad |x'| \to \infty. \tag{2.20}$$

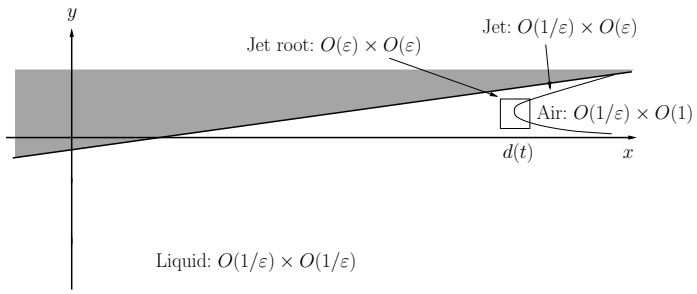

FIG. 2. Proposed asymptotic structure for small-deadrise impact with the inclusion of a cushioning air layer.

2.2 *Asymptotic structure*

We now propose the asymptotic structure illustrated in Figure 2 for the small deadrise angle regime where $0 < \varepsilon \ll 1$. We assume in our analysis that the density ratio, ρ, is also small.

Under these conditions, we expect that the free surface turns over in a small jet-root region (the turnover region) of size of $O(\varepsilon) \times O(\varepsilon)$ on the body, as in the zero-cushioning situation. The liquid is ejected from this region into a slender jet on the body of extent of $O(1/\varepsilon)$ and thickness of $O(\varepsilon)$. At leading order, the main body of the liquid does not see the jet and acts as if it were being loaded by an expanding plate of the extent of the distance between the turnover points, which is of $O(1/\varepsilon)$.

On a horizontal lengthscale of $O(1/\varepsilon)$ and vertical lengthscale of $O(1)$, the air layer is sandwiched between the free surface of the liquid region and the jet/body, as well as filling the cavity in the jet-root region.

We discuss the scalings in the turnover and jet regions in Appendix A. These are important in fully determining the leading-order problem, and we highlight the relevant points when they are required.

2.3 *Leading-order problem*

In the liquid region, we apply Wagner's idea and model the bulk of the impact as an expanding flat plate moving normal to the free surface of the liquid, as in Howison *et al.* (1991). We make the scalings

$$(x',y') = \frac{1}{\varepsilon}(x,y), \quad d' = \frac{d}{\varepsilon}, \quad \phi' = \frac{1}{\varepsilon}\phi, \quad p' = \frac{1}{\varepsilon}p, \quad h'_- = h, \quad t' = t.$$

In the air region, the near flatness of the impactor means that there is an order of magnitude difference between horizontal and vertical lengthscales. The corresponding scales are given by

$$x' = \frac{1}{\varepsilon}x, \quad y' = \hat{y}, \quad \Phi = \frac{1}{\varepsilon^2}\Phi \quad P' = \frac{1}{\varepsilon^2}P \quad h'_- = h, \quad h'_+ = \varepsilon h_+, \quad t' = t.$$

Under these scalings, the dynamic boundary condition on the lower free surface is given by

$$p = \lambda P,$$

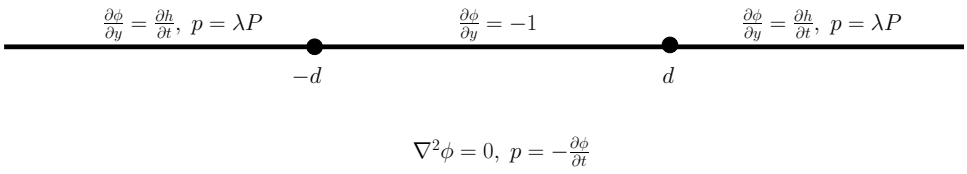

FIG. 3. Leading-order problem in the liquid. The boundary conditions on the body and the free surface linearise onto $y = 0$. The kinematic condition on the impactor is applied for $|x| < d(t)$ and the kinematic and dynamic boundary conditions on the free surface are applied for $|x| > d(t)$. In addition, the initial conditions are given by $\phi(x,y,0) = 0$, $h(x,0) = 0$ and $d(0) = 0$, and the far-field conditions are given by $\phi = (Q_1/\pi)\log r + o(1)$ as $r \to \infty$ and $h = o(1/x)$ as $|x| \to \infty$. As noted in §A2, we require $\phi = O\left(((x \pm d)^2 + y^2)^{1/4}\right)$ as $(x \pm d)^2 + y^2 \to 0$. The problem is closed by (2.21), as described in the text.

where $\lambda = \rho/\varepsilon$. This key parameter is a measure of the relative importance of the density difference between the air and liquid, and the flatness of the body profile characterised by the deadrise angle. In the current analysis, we shall assume that $\lambda \lesssim O(1)$, but in order for the air pressure to enter the leading-order problem, we are also forced to assume that $\varepsilon \ll \lambda$. We will find that λ plays a critical role in determining the value of the coefficients of the sources in (2.17)–(2.18).

Under the above scalings, the leading-order problem for the velocity potential in the liquid linearises into the half-space problem displayed in Figure 3. The problem is completed by noting that the above scalings and the local scalings given in Appendix A enforce that the Wagner condition must hold, as argued in Howison *et al.* (1991). Thus, we require:

$$h(\pm d(t), t) = f(d(t)) - t, \tag{2.21}$$

thereby ensuring that the leading-order free surface meets the impactor at the turnover points.

2.3.1 Conservation of mass

We also note that, by Green's theorem

$$0 = \int_d^\infty \frac{\partial h}{\partial t}\,\mathrm{d}x - 2d + \int_{-\infty}^{-d} \frac{\partial h}{\partial t}\,\mathrm{d}x + Q_1(t).$$

Using the symmetry of the problem and (2.21), we deduce that

$$0 = \frac{\partial}{\partial t}\left[\int_{d(t)}^\infty h(x,t)\,\mathrm{d}x + \frac{1}{2}\int_0^t Q_1(\tau)\,\mathrm{d}\tau - t d(t)\right] + \dot{d}(t) f(d(t)). \tag{2.22}$$

2.3.2 Leading-order air problem

Under the assumption that the jet can be ignored in the leading-order air problem, the kinematic condition on the upper free surface simply reduces to the kinematic condition on the body and, as noted in Appendix A, the dynamic boundary condition is dominated by the jet pressure to leading order. In the air layer it is easier to work with the velocity components in the x- and $\hat{y}$-directions, denoted by $U(x,\hat{y},t)$ and $V(x,\hat{y},t)$ respectively. Here, by symmetry, we need only consider the air layer for $x > d(t)$.

Under the above scalings, the leading-order problem is given by the scaled Euler equations

$$\varepsilon^2\left(\frac{\partial U}{\partial t}+U\frac{\partial U}{\partial x}\right)+V\frac{\partial U}{\partial \hat{y}} = -\varepsilon^2\frac{\partial P}{\partial x}, \tag{2.23}$$

$$\varepsilon^2\left(\frac{\partial V}{\partial t}+U\frac{\partial V}{\partial x}\right)+V\frac{\partial V}{\partial \hat{y}} = -\varepsilon^2\frac{\partial P}{\partial \hat{y}}, \tag{2.24}$$

$$\varepsilon^2\frac{\partial U}{\partial x}+\frac{\partial V}{\partial \hat{y}} = 0, \tag{2.25}$$

$$\frac{\partial U}{\partial \hat{y}}-\frac{\partial V}{\partial x} = 0, \tag{2.26}$$

for $x > d(t)$, $h(x,t) < \hat{y} < f(x)-t$. The kinematic condition on the body is given by,

$$V = \varepsilon^2(-1+f'(x)U) \quad \text{on} \quad \hat{y} = f(x)-t,\ x > d(t) \tag{2.27}$$

while on the free surface it is given by

$$V = \varepsilon^2\left(\frac{\partial h}{\partial t}+U\frac{\partial h}{\partial x}\right) \quad \text{on} \quad \hat{y} = h(x,t),\ x > d(t). \tag{2.28}$$

The dynamic boundary condition is

$$p = \lambda P \quad \text{on} \quad \hat{y} = h(x,t),\ x > d(t). \tag{2.29}$$

If we expand in powers of ε^2, it is simple to deduce that to leading-order

$$U_0(x,\hat{y},t) = U(x,t), \quad V_0(x,\hat{y},t) = 0, \quad P_0(x,\hat{y},t) = P(x,t), \tag{2.30}$$

where a subscript zero denotes a leading-order variable. Thus, from (2.23),

$$\frac{\partial U}{\partial t}+U\frac{\partial U}{\partial x} = -\frac{\partial P}{\partial x}. \tag{2.31}$$

Moreover, we can integrate the $O(\varepsilon^2)$ terms in (2.25) across the air layer and apply (2.27)–(2.28) to deduce the usual squeeze-film conservation equation

$$\frac{\partial}{\partial t}\left(f(x)-t-h\right)+\frac{\partial}{\partial x}\left(\left(f(x)-t-h\right)U\right) = 0. \tag{2.32}$$

In Appendix A, we show that U must be bounded as $x \to d(t)$. In particular, we deduce that

$$U(d(t),t) = \dot{d}(t). \tag{2.33}$$

Therefore, the air flow is governed by (2.31)–(2.32) subject to (2.21), (2.33) and the far-field condition, which we discuss in more detail in §2.3.4.

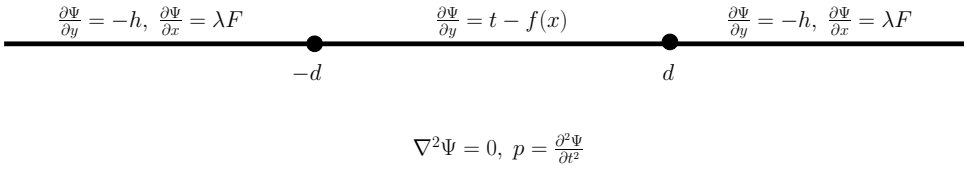

FIG. 4. Leading-order problem for the displacement potential, Ψ. The initial condition is given by $d(0) = 0$ and the far-field conditions are given by $\Psi = -(\int_0^t Q_1(\tau)\,\mathrm{d}\tau/2\pi)\log r + o(1)$ as $r \to \infty$ and $h = o(1/x)$ as $|x| \to \infty$. The smoothing effect of the integral in (2.34) means that we require $\Psi = O\left(|z \mp d|^{3/2}\right)$ as $z \to \pm d$.

2.3.3 Leading-order liquid problem

As in Korobkin (1988), it is convenient to define the leading-order displacement potential in the liquid by

$$\Psi = -\int_0^t \phi\,(x,y,\tau)\,\mathrm{d}\tau. \tag{2.34}$$

Using the leading-order form of Bernoulli's equation as shown in Figure 4, we see that $\partial p/\partial x = \partial^3\Psi/\partial t^2\partial x$. The dynamic boundary condition and (2.31) give

$$\frac{\partial^3\Psi}{\partial t^2\partial x} = \lambda\frac{\partial P}{\partial x} = -\lambda\left(\frac{\partial U}{\partial t} + U\frac{\partial U}{\partial x}\right)$$

Therefore, if we write

$$\frac{\partial\Psi}{\partial x} = \lambda F \quad \text{on} \quad y = 0,\ |x| > d(t),$$

then

$$F = \int_0^t \int_0^\tau \frac{\partial P}{\partial x}(x,s)\,\mathrm{d}s\mathrm{d}\tau,$$

where the functions of integration in the first equation have been chosen to meet the conditions that $\Psi = \partial\Psi/\partial t = 0$ at $t = 0$. Note that, by the symmetry of the problem, the function $F(x,t)$ is odd in x.

Hence, under the transformation (2.34), the leading-order liquid problem transforms to that shown in Figure 4, where we have written $z = x + \mathrm{i}y$. Note that $\partial\Psi/\partial y$ is continuous at the turnover points by the Wagner condition (2.21). Solving this Riemann-Hilbert problem, we deduce that

$$\frac{\mathrm{d}\Upsilon}{\mathrm{d}z} = -\frac{\mathrm{i}\sqrt{z^2-d^2}}{\pi}\left[\int_{-\infty}^{-d}\frac{\lambda F(\zeta,t)}{\sqrt{\zeta^2-d^2}(\zeta-z)}\,\mathrm{d}\zeta - \int_{-d}^{d}\frac{t-f(\zeta)}{\sqrt{d^2-\zeta^2}(\zeta-z)}\,\mathrm{d}\zeta - \int_{d}^{\infty}\frac{\lambda F(\zeta,t)}{\sqrt{\zeta^2-d^2}(\zeta-z)}\,\mathrm{d}\zeta\right],$$

where $\Upsilon = \Psi + \mathrm{i}\chi$ and χ is the harmonic conjugate to Ψ. This solution automatically satisfies the Wagner condition (2.21) while the consistency condition

$$\frac{1}{\pi}\int_{-d}^{d}\frac{t-f(\zeta)}{\sqrt{d^2-\zeta^2}}\,\mathrm{d}\zeta + \frac{2\lambda}{\pi}\int_{d}^{\infty}\frac{F(\zeta,t)}{\sqrt{\zeta^2-d^2}}\,\mathrm{d}\zeta = 0 \tag{2.35}$$

guarantees that $\mathrm{d}\Upsilon/\mathrm{d}z = O(1/z)$ as $z \to \infty$.

We can evaluate this solution as $(z-x)/\mathrm{i} \uparrow 0$, $x > d(t)$ to deduce that

$$h(x,t) = \frac{\sqrt{x^2-d^2}}{\pi} \int_{-d}^{d} \frac{t - f(\zeta)}{\sqrt{d^2-\zeta^2}(\zeta - x)}\,\mathrm{d}\zeta + \frac{2\lambda x\sqrt{x^2-d^2}}{\pi} \barint_{d}^{\infty} \frac{F(\zeta,t)}{\sqrt{\zeta^2-d^2}(\zeta^2-x^2)}\,\mathrm{d}\zeta,$$

where the dash indicates that the integral is defined in the Cauchy principal value sense. Note that (2.35) ensures that $h \to 0$ as $x \to \infty$ and that if $\lambda = 0$, this is simply the Wagner solution for h.

Equation (2.35) allows us to determine the leading-order location of the turnover point, $d(t)$ in terms of the air pressure gradient. We can make the change of variables $\zeta = d\sin\theta$ in the first integral and $\zeta = d\cosh\psi$ in the second integral of (2.35) to deduce that

$$\frac{\pi t}{2} = \int_0^{\pi/2} f(d\sin\theta)\,\mathrm{d}\theta - \lambda \int_0^{\infty} F(d\cosh\psi, t)\,\mathrm{d}\psi, \tag{2.36}$$

where we have used the fact that $f(x)$ is even.

2.3.4 Summary

Thus, defining

$$\bar{Q}_1(t) = \int_0^t Q_1(\tau)\,\mathrm{d}\tau,$$

for $x > d(t)$, our air-cushioning model for the unknowns $h, F, U, d, \bar{Q}_1$ comprises:

$$h(x,t) = \frac{\sqrt{x^2-d^2}}{\pi} \int_{-d}^{d} \frac{t - f(\zeta)}{\sqrt{d^2-\zeta^2}(\zeta - x)}\,\mathrm{d}\zeta + \frac{2\lambda x\sqrt{x^2-d^2}}{\pi} \barint_{d}^{\infty} \frac{F(\zeta,t)}{\sqrt{\zeta^2-d^2}(\zeta^2-x^2)}\,\mathrm{d}\zeta, \tag{2.37}$$

$$0 = \frac{\partial}{\partial t}\left(f(x) - t - h\right) + \frac{\partial}{\partial x}\left(\left(f(x) - t - h\right)U\right), \tag{2.38}$$

$$F(x,t) = -\int_0^t \int_0^\tau \frac{\partial U}{\partial t}(x,s) + U(x,s)\frac{\partial U}{\partial x}(x,s)\,\mathrm{d}s\mathrm{d}\tau, \tag{2.39}$$

$$\frac{\pi t}{2} = \int_0^{\pi/2} f(d\sin\theta)\,\mathrm{d}\theta - \lambda \int_0^{\infty} F(d\cosh\psi, t)\,\mathrm{d}\psi, \tag{2.40}$$

$$0 = \frac{\partial}{\partial t}\left[\int_{d(t)}^{\infty} h(x,t)\,\mathrm{d}x + \frac{\bar{Q}_1(t)}{2} - t d(t)\right] + \dot{d}(t) f(d(t)), \tag{2.41}$$

together with the boundary condition

$$U(d(t),t) = \dot{d}(t), \tag{2.42}$$

and the far-field conditions that

$$U(x,t) = \frac{Q_2(t)}{\pi x} + o\left(\frac{1}{x}\right), \quad h(x,t) = o\left(\frac{1}{x}\right) \quad \text{as} \quad x \to \infty. \tag{2.43}$$

We expect the solution of this system to differ from that of the full model by $O(\varepsilon)$ as $\varepsilon \to 0$, except in the turnover regions. As in the uncushioned case, new expansions are needed in these regions, in which $x - d \sim y - \varepsilon(f(d) - t) \sim O(\varepsilon^2)$ as described in detail in Appendix A. It transpires that, as long as $\rho \ll 1$, the liquid flow in these regions is unaffected by the air flow to lowest order, and that the air moves with the uniform velocity (2.42) in the x-direction.

3. Solutions for $\lambda \ll 1$

We now consider impacts where the effect of the air-cushioning layer is small, that is $\lambda \ll 1$. We can proceed to terms of $O(\lambda)$ under the assumption that $\varepsilon \ll \lambda \ll 1$; if $\lambda = O(\varepsilon)$ as $\varepsilon \to 0$, the air cushioning enters the second-order problem described in Oliver (2007), a distinguished limit we shall not pursue here.

Therefore, we seek a small-λ perturbation of the system (2.37)–(2.41) of the form

$$h = h_0 + \lambda h_1 + O(\lambda^2), \quad U = U_0 + \lambda U_1 + O(\lambda^2), \quad F = F_0 + \lambda F_1 + O(\lambda^2), \quad d = d_0 + \lambda d_1 + O(\lambda^2)$$

as $\lambda \to 0$. We also write

$$\bar{Q}_1 = \lambda \bar{Q}_{10}(t) + \lambda^2 \bar{Q}_{11}(t) + O(\lambda^3), \quad Q_2(t) = Q_{20}(t) + \lambda Q_{21}(t) + O(\lambda^2)$$

as $\lambda \to 0$. We observe immediately that (2.37) reduces to the Wagner solution

$$h_0(x,t) = \frac{\sqrt{x^2 - d_0(t)^2}}{\pi} \int_{-d_0}^{d_0} \frac{t - f(\zeta)}{\sqrt{d_0(t)^2 - \zeta^2}(\zeta - x)} \,\mathrm{d}\zeta, \tag{3.1}$$

where, from (2.41), $d_0(t)$ is given by the classical Wagner formula

$$\frac{\pi t}{2} = \int_0^{\pi/2} f(d_0(t)\sin\theta)\,\mathrm{d}\theta. \tag{3.2}$$

Therefore, by (2.38),

$$U_0(x,t) = \frac{1}{f(x) - t - h_0(x,t)} \left[x - d_0(t) + \int_{d_0}^{x} \frac{\partial h_0}{\partial t}(\zeta,t)\,\mathrm{d}\zeta \right]. \tag{3.3}$$

The function $F_0(x,t)$ can then be determined in principle from the leading-order form of (2.39). We note that, once we know $F_0(x,t)$, from (2.40) we can simply write down that the $O(\lambda)$ correction to position of the turnover region as

$$d_1(t) = \frac{\int_0^\infty F_0(d_0(t)\cosh\psi, t)\,\mathrm{d}\psi}{\int_0^{\pi/2} f'(d_0\sin\theta)\sin\theta\,\mathrm{d}\theta}, \tag{3.4}$$

where here a prime indicates differentiation with respect to argument. Note that the denominator can be simplified using (3.2) as

$$\int_0^{\pi/2} f'(d_0\sin\theta)\sin\theta\,\mathrm{d}\theta = \frac{\pi}{2\dot{d}_0(t)}. \tag{3.5}$$

3.1 *Parabolic impactors*

Analytic progress is possible when the impactor is given by

$$f(x) = \frac{x^2}{2}. \tag{3.6}$$

Then, (3.1) and (3.2) can be trivially integrated to find well-known Wagner solution for parabolic impact, given by

$$h_0(x,t) = \frac{x^2}{2} - t - \frac{|x|}{2}\sqrt{x^2 - d_0(t)^2}, \quad d_0(t) = 2\sqrt{t}. \tag{3.7}$$

Utilising these expressions, the horizontal component of air velocity can be found from (3.3) to be

$$U_0(x,t) = \frac{2}{x}. \tag{3.8}$$

This result is independent of λ as long as $\varepsilon \ll \lambda \ll 1$ and it is consistent with (2.42).

Using (3.8) in (2.18) gives $Q_{20} = 2\pi$. Thus, as we let $x \to \infty$ and move out of the small deadrise region, the velocity potential in the air must have a logarithmic singularity. In contrast, the air pressure does not have this logarithmic behaviour at infinity; we can use (3.8) and (2.31) to show that

$$P_0 = -\frac{2}{x^2}. \tag{3.9}$$

Furthermore, the leading-order velocity potential in the liquid has no such source term in the far-field.

Upon integrating (3.8) we deduce that

$$F_0(x,t) = \frac{2t^2}{x^3}, \tag{3.10}$$

which is strictly positive for all $x > d_0(t)$. We can now work out the correction to the turnover point location by utilising (3.4), which gives

$$d_1(t) = \frac{1}{8}. \tag{3.11}$$

Therefore, even though the correction to the turnover point location places it further from the initial point of impact, the turnover point speed remains the same as that for uncushioned impact.

In order to determine $\bar{Q}_{10}$, we require the correction to the Wagner free surface. From (2.37), we find that

$$h_1(x,t) = \frac{x\sqrt{t}}{8\sqrt{x^2-4t}} - \frac{\sqrt{t}(x^2+8t)\sqrt{x^2-4t}}{8x^3}. \tag{3.12}$$

The $O(\lambda)$ terms in (2.41) give

$$0 = \frac{\bar{Q}_{10}(t)}{2} + \frac{t}{8} + \int_{2\sqrt{t}}^{\infty} h_1(x,t)\,\mathrm{d}x + \frac{\partial}{\partial d}\left(\int_d^{\infty} h_0(x,t)\,\mathrm{d}x\right)\bigg|_{d=2\sqrt{t}},$$

so that

$$\bar{Q}_{10}(t) = \frac{7t}{4}. \tag{3.13}$$

The leading-order solution in the Wagner region presented here does not describe the flow when $t = O(\lambda^2)$ as $\lambda \to 0$, there then being a nonuniformity in the expansion of d. Unfortunately, when we rescale for small times by writing

$$(x,y,\zeta) = \lambda\left(\tilde{x},\tilde{y},\tilde{\zeta}\right), \quad d = \lambda\tilde{d}, \quad (s,\tau,t) = \lambda^2(\tilde{s},\tilde{\tau},\tilde{t}), \quad h = \lambda^2\tilde{h}, \quad U = \frac{\tilde{U}}{\lambda}, \quad F = \lambda\tilde{F}, \quad \bar{Q}_1 = \frac{\tilde{\bar{Q}}_1}{\lambda^2},$$

we retrieve (2.37)-(2.41) with $\lambda = 1$. In general this system must be tackled numerically.

3.2 *Implication for circular cylinder impacts*

Consider the impact of the circular cylinder with cross-section given in dimensional variables by

$$(y^* - R + V_0 t^*))^2 + x^{*2} = R^2, \tag{3.14}$$

where R is the radius of the circle, which we assume is large compared to the penetration depth, L. We wish to consider the outer air flow caused by the penetration of the circle into the liquid on the penetration timescale of L/V_0, where $L/R \ll 1$. On this scale, the free surface of the liquid is seen as flat to leading order in the air. Thus, if we set

$$x^* = RX, \quad y^* = RY, \quad t^* = \frac{L}{V_0} t',$$

we consider perturbations to the air motion on the scale of the radius of the circle, so that

$$\Phi^* = RV_0 \Phi', \quad P^* = \rho_a V_0^2 P,$$

and perturbations to the liquid motion on the scale of the penetration depth,

$$\phi^* = LV_0 \phi', \quad p^* = \rho_l V_0^2 p, \quad h^* = \frac{L^2}{R} h'.$$

Therefore, using a subscript zero to indicate a leading order variable, the flow in the air is given by the Neumann problem

$$\nabla^2 \Phi_0' = 0 \quad \text{in the air,} \tag{3.15}$$

$$\frac{\partial \Phi_0'}{\partial Y} = 0 \quad \text{on} \quad y' = 0, \tag{3.16}$$

$$\frac{\partial \Phi_0'}{\partial Y} = -1 + X \frac{\partial \Phi_0'}{\partial X} + \left(1 + \frac{\partial \Phi_0'}{\partial Y}\right) Y \quad \text{on} \quad (Y-1)^2 + X^2 = 1. \tag{3.17}$$

Now, if we also assume $\lambda \ll 1$, then to leading order in λ, the flow in the liquid is unaffected by the air flow and is thus the dipole flow that is the far-field of the solution of the problem in Figure 3. In this flow, P is of $O(1)$ and hence the boundary condition $p \sim \lambda P$ on $Y = 0$ is automatically satisfied to leading order in ε.

We note that a solution of (3.15)–(3.17) must satisfy

$$\frac{\partial \Phi_0'}{\partial R} \sim \frac{2}{R} \quad \text{as} \quad R = \sqrt{X^2 + Y^2} \to 0,$$

so that any solution to this outer air problem automatically matches with the Wagner solution described in §3.1.

As in the classical theory of cushioning between rigid impactors described in, for example, Jeffery (1912) and Czaykowski (1970), we can set

$$\xi + \mathrm{i}\eta = \frac{2\mathrm{i}}{X + \mathrm{i}Y} \tag{3.18}$$

to transform the problem for Φ_0' into

$$\frac{\partial^2 \Phi_0'}{\partial \xi^2} + \frac{\partial^2 \Phi_0'}{\partial \eta^2} = 0 \quad \text{for} \quad 0 < \xi < 1, \ -\infty < \eta < \infty; \tag{3.19}$$

here $\xi = 0$ is $Y = 0$ and $\xi = 1$ is the impactor. The conditions (3.16)–(3.17) transform to

$$\frac{\partial \Phi_0'}{\partial \xi} = 0 \quad \text{on} \quad \xi = 0, \tag{3.20}$$

$$\frac{\partial \Phi_0'}{\partial \xi} = \frac{2(1-\eta^2)}{(1+\eta^2)^2} \quad \text{on} \quad \xi = 1, \tag{3.21}$$

and we require Φ_0' to only grow logarithmically as $\eta \to \infty$. Note that, due to the symmetry of the problem, we can simply consider $\eta > 0$ with the condition that

$$\frac{\partial \Phi_0'}{\partial \eta} = 0 \quad \text{on} \quad \eta = 0. \tag{3.22}$$

We can solve the problem in the strip by using the appropriate Green's function. We deduce that

$$\frac{\partial \Phi_0'}{\partial \xi}(\xi,\eta) = \frac{1}{2\pi}\int_{-\infty}^{\infty} \frac{2(1-s^2)}{(1+s^2)^2} \int_{-\infty}^{\infty} \mathrm{e}^{-\mathrm{i}k(s-\eta)} \frac{\sinh k\xi}{\sinh k}\,\mathrm{d}k\,\mathrm{d}s. \tag{3.23}$$

However, we can deduce the far-field flow from the fact that as $\eta \to \infty$,

$$\frac{\partial \Phi_0'}{\partial \xi} = 0 \quad \text{on} \quad \xi = 0, \quad \frac{\partial \Phi_0'}{\partial \xi} \sim -\frac{2}{\eta^2} \quad \text{on} \quad \xi = 1,$$

Hence,

$$\frac{\partial \Phi_0'}{\partial \xi} \sim -\frac{2\xi}{\eta^2} \quad \text{as} \quad \eta \to \infty, \tag{3.24}$$

and therefore

$$\Phi_0' \sim -\frac{\xi^2}{\eta^2} + F(\eta) \quad \text{as} \quad \eta \to \infty, \tag{3.25}$$

where we can determine $F(\eta)$ by applying conservation of mass. A simple application of Green's theorem gives us that

$$0 = \int_0^1 \frac{2\xi^2}{\eta^3} + \frac{\mathrm{d}F}{\mathrm{d}\eta}\,\mathrm{d}\xi + \frac{2\eta}{1+\eta^2} \quad \text{as} \quad \eta \to \infty,$$

so that upon integrating and expanding, we must have

$$F(\eta) \sim -2\log\eta + o(\log\eta).$$

Hence we see that Φ_0' has the desired far-field behaviour.

4. Impact of a wedge

We now consider the infinite wedge given in dimensional coordinates by

$$\frac{y^*}{L} = \varepsilon\left|\frac{x^*}{L}\right| - \frac{V_0}{L}t^*.$$

As there is no natural lengthscale in the wedge impact problem, we can find a similarity form of (2.37)–(2.41) by scaling

$$\eta = \frac{x}{\alpha t}, \quad \xi = \frac{y}{t}, \quad \zeta = \frac{\chi}{\alpha t}, \quad d = \alpha t, \quad h = t h^\dagger(\eta), \quad U = U^\dagger(\eta), \quad F = tF^\dagger(\eta), \quad \bar{Q}_1^\dagger = \bar{Q}_1 t^2;$$

here α, the speed of the turnover point, has been introduced for convenience. Under this transformation and omitting the algebraic manipulation in (2.39), we find

$$h^\dagger(\eta) = -1+\frac{2\alpha\eta}{\pi}\arcsin\left(\frac{1}{\eta}\right)+\frac{2\lambda\eta}{\pi}\sqrt{\eta^2-1}\fint_1^\infty \frac{F^\dagger(\chi)}{\sqrt{\chi^2-1}(\chi^2-\eta^2)}\,\mathrm{d}\chi, \tag{4.1}$$

$$U^\dagger(\eta) = \frac{\alpha}{\alpha\eta-1-h^\dagger(\eta)}\left[(1-h^\dagger(\eta))\eta+\alpha-2+\int_1^\eta h^\dagger(\chi)\,\mathrm{d}\chi\right], \tag{4.2}$$

$$F^\dagger(\eta) = 1-\eta\int_\eta^\infty \frac{U^\dagger(\chi)}{\chi^2}\,\mathrm{d}\chi-\frac{1}{\alpha}\int_\eta^\infty \frac{\chi-2\eta}{2\chi^3}U^\dagger(\chi)^2\,\mathrm{d}\chi, \tag{4.3}$$

$$0 = \frac{\pi}{2}-\alpha+\lambda\int_0^\infty F^\dagger(\cosh\psi)\,\mathrm{d}\psi, \tag{4.4}$$

$$0 = \alpha\int_1^\infty h^\dagger(\eta)\,\mathrm{d}\eta+\frac{\lambda Q_1^\dagger}{2}-\alpha+\frac{\alpha^2}{2}. \tag{4.5}$$

Henceforth, we drop the dagger notation indicating the similarity variables. In the regime where $\lambda \ll 1$, we can use (4.1) and (4.4) to deduce that the leading-order (in λ) free surface profile and leading-order position of the turnover point are given by the well-known wedge-entry problem results

$$h_0(\eta) = -1+\eta\arcsin\frac{1}{\eta} \quad \text{and} \quad \alpha_0 = \frac{\pi}{2}. \tag{4.6}$$

In the far-field, this has the characteristic Wagner behaviour

$$h_0 \sim \frac{1}{6\eta^2}+\ldots \quad \text{as} \quad \eta\to\infty. \tag{4.7}$$

We can integrate (4.2) to deduce that

$$U_0(\eta) = \frac{\sqrt{\eta^2-1}}{\eta-(2/\pi)\eta\arcsin(1/\eta)}. \tag{4.8}$$

Hence, the tangential component of air velocity now has the expansion

$$U_0(\eta) \sim 1+\frac{2}{\pi\eta}+\ldots \quad \text{as} \quad \eta\to\infty, \tag{4.9}$$

so that in the example of a wedge, we were not conservative enough in our far-field expansion in the air. We must in fact include a rigid-body motion as well as the source-like singularity. Note also that now $Q_2 = \pi$ to leading-order. Moreover, the air pressure also has a logarithmic singularity in the far field. This suggests that the leading-order form of the dynamic boundary condition, which is given by

$$p_0 = 0,$$

breaks down as $\eta\to\infty$. Thus we must match this solution with an outer region where the dynamic boundary condition is rescaled. We will discuss this shortly.

We can calculate $P_0(\eta)$ and $F_0(\eta)$ from (2.31) and (4.3) respectively. There is not a simple closed form for either, but we can solve for them numerically. We plot the results in Figure 5. Furthermore, we

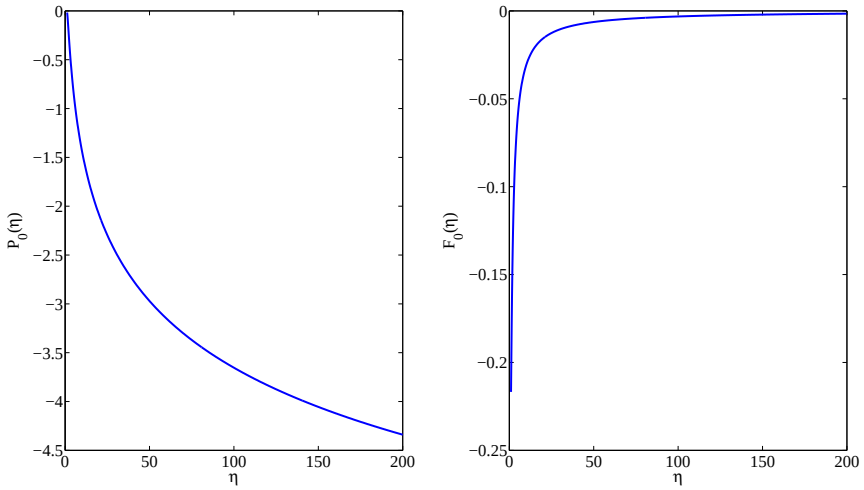

FIG. 5. $P_0(\eta)$ (left) and $F_0(\eta)$ (right). There is a logarithmic singularity in the pressure in the far-field, so that the pressure becomes negative and infinite as $\eta \to \infty$. As a result of this singularity, $F_0(\eta)$ is a strictly negative function.

can use (4.4) to solve for the $O(\lambda)$ correction to the turnover point location by noting that

$$\alpha_1 = \left[\int_0^\infty F_0\left(\frac{\pi}{2}\cosh\psi\right)\mathrm{d}\psi\right].$$

We can evaluate this numerically and we find that $\alpha_1 = -0.403$ to three significant figures. In contrast to the parabola impact, the turnover point speed is lower than the Wagner turnover point speed.

It is simple to substitute (4.9) into (4.3) to show that

$$F_0 \sim -\frac{1}{\pi\eta} + \left(\frac{1}{6} - \frac{2}{3\pi^2}\right)\frac{1}{\eta^2} + \ldots \quad \text{as} \quad \eta \to \infty, \tag{4.10}$$

so that upon substituting into the $O(\lambda)$ form of (4.1), we see that

$$h_1(\eta) = \frac{b}{\eta^2}\log\eta + \frac{c}{\eta^2} + o\left(\frac{1}{\eta^2}\right) \quad \text{as} \quad \eta \to \infty, \tag{4.11}$$

where

$$b = -\frac{2}{\pi}\left(\frac{1}{6} - \frac{2}{3\pi^2}\right), \tag{4.12}$$

$$c = \frac{\alpha_1}{3\pi} + \frac{1}{\pi}\int_1^\infty \frac{F_0(\chi)}{\sqrt{\chi^2-1}}\mathrm{d}\chi - \frac{2}{\pi^2} - \frac{2}{\pi}\int_1^\infty \frac{\chi^2 F_0(\chi)}{\sqrt{\chi^2-1}} + \frac{1}{\pi} + \frac{2}{\pi}\left(\frac{1}{6} - \frac{2}{3\pi^2}\right)\frac{1}{\chi}\mathrm{d}\chi. \tag{4.13}$$

Therefore there is a nonuniformity in h as we move far away from the point of impact. The form of h_1 suggests that the asymptotic analysis of (4.1)–(4.5) may need to be reconsidered when $\log\eta = O(1/\lambda)$

and that in such a region h will contain terms involving η^{λ}. As the nonuniformity occurs when $\log\eta = O(1/\lambda)$, by definition this corresponds to a nonuniformity both for large x when $t = O(1)$ and for small t when $x = O(1)$.

5. Conclusion

We have used Wagner theory to derive a model for air-cushioning in constant-velocity, two-dimensional impacts into a half-space of ideal liquid. Under the assumption that the air is also ideal, we have employed the displacement potential to write down the local model for impact under the assumption that the impactor is nearly flat, that is the deadrise angle, ε, of the impactor is small. The local turnover flow is the same as that for Wagner theory provided that the density ratio, ρ, between the air and liquid is small, which enables us to solve the resulting inner problem in the air and use the Wagner condition for the free surface in the leading-order displacement potential problem.

This has enabled us to deduce the integro-differential system in §2.3.4 for the leading-order free surface profile, leading-order x-component of velocity in the air and a function, F, which depends upon the leading-order pressure gradient in the air. Our model assumed that the parameter $\lambda = \rho/\varepsilon$ is at most order unity and that the free surface is integrable.

In order to make analytic progress on the resulting system, we considered the physically-relevant liquid-air regime where λ is small. To leading-order, the solution is simply that given by the well-known Wagner theory. We derived a general expression for the correction to the turnover point location due to the influence of the air layer and a conservation-of-mass analysis forced us to conclude that the velocity potential in the liquid must admit a logarithmic term in the far-field, something that is not seen in Wagner theory. We proceeded to consider two specific examples of impact to highlight the novelties of the solution.

Firstly, we discussed the impact of a circular cylinder, which is approximated locally by a parabola. We derived the leading-order air velocity and the function F, which enabled us to state the first-order correction to the free surface profile and the correction to the turnover point location. While the speed of the turnover point remained unchanged from its value in Wagner theory, the turnover point is displaced slightly further from the initial point of impact. This indicated that the model breaks down for small times where $t = O(\lambda^2)$ when we must solve the full integro-differential system (provided that $\varepsilon \ll \lambda^2$). We noted that the leading-order velocity potential in the air must have a source-like singularity in the far-field and thus the parabola model also breaks down at large distances away from the point of impact, where the deadrise angle is no longer small and the impactor is circular. In this regime, the air flow around the cylinder is driven by a logarithmic singularity at the point where the circle touches the free surface, so that this is the outer flow to which we needed to match our Wagner-type solution.

The second example we considered was that of symmetric wedge impact. In this case, our system of integro-differential equations is in similarity form with only one independent variable and the leading-order forms of the air velocity and the function F were readily derived from the Wagner solution. We noted that for the wedge, the function F was strictly negative, as opposed to being strictly positive as in the case of the parabola. Due to this, the turnover speed was found to be slower than that for Wagner theory. In the far-field, we noted that there was both a rigid-body term and a logarithmic term in the expansion of the air velocity potential. Moreover, a nonuniformity was found in the form of a $(/x^2)\log x$ term in the far-field expansion of the free surface.

We conclude by mentioning that the displacement potential formulation could be applied to the pre-touchdown flow when the air gap is nonzero for all x. This may be useful in numerical simulations of this problem as considered, for example, by Smith *et al.* (2003) and Purvis & Smith (2004).

Funding

This work was supported in part by Award No. KUK-C1-013-04, made by King Abdullah University of Science and Technology (KAUST), an Engineering and Physical Sciences Research Council studentship (M.R.M.) and a Leverhulme Emeritus Fellowship (J.R.O.).

Acknowledgements

The authors would like to thank Prof. S.D. Howison for helpful discussions.

A Turnover & jet region scalings

In order to fully formulate the problem in the liquid, and hence evaluate the influence of the air on the Wagner solution, it is necessary to consider the flow in the jet-root region. We aim to show that the air can be neglected to leading order and hence the Helmholtz solution in Wagner theory prevails. By symmetry, we only consider the right-hand jet root, about the turnover point $x' = d'(t')$.

A1 *Turnover region: liquid*

In the liquid, we apply the Wagner scalings as given in, for example, Howison *et al.* (1991). Thus, we scale:

$$x' = \frac{d(t)}{\varepsilon} + \varepsilon\bar{x} \quad y' = (f(d(t)) - t) + \varepsilon\bar{y}, \quad d'(t') = \frac{d(t)}{\varepsilon}$$

This is a travelling-wave frame moving with the turnover point. Thus, as the inner region moves with speed of $O(1/\varepsilon)$ in the x'-direction, we must set

$$\phi' = \dot{d}(t)\bar{x} + \bar{\phi}$$

where on the right-hand side we have accounted for the velocity due to the moving frame, so that $\bar{\phi} = 0$ if the fluid were stationary in the lab frame. A dot indicates differentiation with respect to time. The multivalued free surface is defined as $\bar{y} = \bar{h}(\bar{x}, t)$, where

$$h' = (f(d(t)) - t) + \varepsilon\bar{h}.$$

Finally, from Bernoulli's equation, we deduce that the pressure is scaled by

$$p' = \frac{1}{\varepsilon^2}\bar{p}.$$

A2 *Turnover region: air*

By similar arguments, the length scales in the jet-root air region are identical to those in the jet-root liquid region. The potential scale is given by

$$\Phi' = \dot{d}(t)\bar{x} + \bar{\Phi}.$$

Thus, the pressure scale is given by

$$P' = \frac{1}{\varepsilon^2}\bar{P}.$$

Therefore, under the scalings in §A1 and the above, we deduce that the dynamic boundary condition in the inner region is given by

$$\bar{p} = \rho \bar{P}. \tag{A1}$$

Hence, as we are assuming that $\rho \lesssim O(\varepsilon)$ throughout our analysis, we deduce that to leading-order (in ε), the dynamic boundary condition is given by $\bar{p} = 0$.

Using this observation and by performing a standard asymptotic expansion of the inner region problem, it is simple to show that to leading order, the flow in the liquid collapses directly to the standard Helmholtz flow as presented for Wagner theory in Howison *et al.* (1991). Furthermore, the upper free surface (i.e. that which can be thought of as the jet) asymptotes to $\bar{h} \sim -J(t)$ for some function $J(t)$ as $\bar{x} \to \infty$ and the lower free surface asymptotes to $\bar{h} \sim -4\sqrt{J(t)/\pi}\sqrt{\bar{x}}$ as $x \to \infty$. In particular, this means that ϕ, h must have square-root behaviour at the turnover points in the 'outer' Wagner problem (cf. Figure 3).

Moreover, at leading order the air flow completely decouples from the Helmholtz flow: given $\bar{h}$, we can solve Laplace's equation in this region subject to the leading-order kinematic boundary condition on the free surface, which is given by

$$\frac{\partial \bar{\Phi}}{\partial \bar{y}} = \frac{\partial \bar{h}}{\partial \bar{x}} \frac{\partial \bar{\Phi}}{\partial \bar{y}} \quad \text{or} \quad \frac{\partial \bar{\Phi}}{\partial \bar{n}} = 0 \quad \text{on} \quad \bar{y} = \bar{h}, \tag{A2}$$

and the matching condition to the 'outer' air region.

We note that a simple application of Green's theorem in the region Γ bounded by the curve $\partial\Gamma$, as shown in Figure 6, allows us to deduce that

$$0 = \iint_{\Gamma} \nabla^2 \bar{\Phi} \, \mathrm{d}S = \int_B^A \frac{\partial \bar{\Phi}}{\partial \bar{x}} \mathrm{d}y, \tag{A3}$$

where we have applied (A2). A and B are defined as the two different values of $\bar{y}$ that for any given $\bar{x}$ satisfy $\bar{y} = \bar{h}(\bar{x}, t)$.

As the 'outer' free surface has square-root behaviour at the turnover point, (2.32) allows us to deduce that U can have, at worst, an inverse square-root singularity as we approach the turnover point, say

$$U = \frac{C(t)}{\sqrt{x - d(t)}} + O(1) \quad \text{as} \quad x \to d(t),$$

where $C(t)$ is an unknown coefficient. Hence, matching with the inner region, we deduce that

$$\frac{\partial \bar{\Phi}}{\partial \bar{x}} \sim \frac{C(t)}{\varepsilon \sqrt{\bar{x}}} \quad \text{as} \quad \bar{x} \to \infty.$$

Thus, upon letting the contour in Figure 6 tend to infinity, we deduce from (A3) that

$$0 = \frac{C(t)}{\varepsilon \sqrt{\bar{x}}}(B - A) = \frac{C(t)}{\varepsilon \sqrt{\bar{x}}} \left(-4\sqrt{\frac{J(t)}{\pi}} \sqrt{\bar{x}} + J(t) \right) \quad \text{as} \quad \bar{x} \to \infty,$$

so that we must demand that $C(t) = 0$.

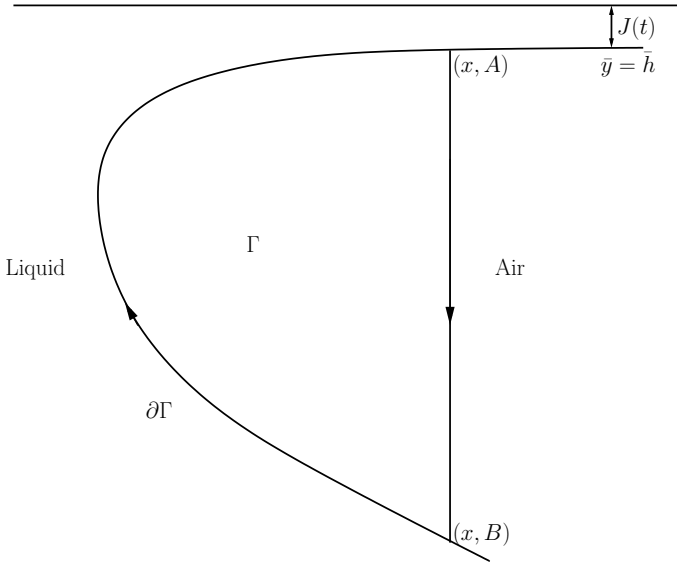

FIG. 6. The contour Γ in the inner-region air cavity.

Furthermore, we can repeat this analysis with the $O(1)$ term of the expansion for U as $x \to d(t)$: if $U \sim D(t)$ as $x \to d(t)$, we deduce that

$$\frac{\partial \bar{\Phi}}{\partial \bar{x}} \sim D(t) - \dot{d}(t) \quad \text{as} \quad \bar{x} \to \infty,$$

and thus assuming the jet has nonzero thickness, we must have $D(t) = \dot{d}(t)$. Thus, the unique solution to the inner air flow is given by

$$\frac{\partial \bar{\Phi}}{\partial \bar{x}} = \frac{\partial \bar{\Phi}}{\partial \bar{y}} = 0. \tag{A4}$$

Hence, the flow in the inner region is entirely due to the moving frame.

A3 *Jet*

Assuming that the jet does not separate, we can make the standard Wagner scalings in the jet, as given in Howison *et al.* (1991), so that the pressure is scaled by

$$\frac{\rho_l V^2}{\varepsilon^2}.$$

In §2.3, we have forced the air and liquid pressures to balance on the free surface, so that

$$\frac{\rho_a V^2}{\varepsilon^2} \sim \frac{\rho_l V^2}{\varepsilon}.$$

Thus, on the free surface of the jet, the jet pressure dominates so that to leading-order the dynamic boundary condition is given by

$$p = 0.$$

Therefore the leading-order jet flow is governed by the zero-gravity shallow water equations and the jet is completely modelled by the Wagner solution, as given in Howison *et al.* (1991).

References

ARMAND, J.-L. & COINTE, R. (1987) Hydrodynamic impact analysis of a cylinder, *ASME J. Offshore Mech. Arc. Eng.*, **111**, 109–114.

CZAYKOWSKI, J.T. (1970) *Some unsteady problems in fluid dynamics.* Thesis (DPhil). University of Oxford.

DE RUITER, J., OH, J.M., VAN DEN ENDE, D. & MUGELE, F. (2012) Dynamics of collapse of air films in drop impact, *Phys. Rev. Lett.*, **108** (7), 074505.

DRISCOLL. M.M. & NAGEL, S.R. (2011) Ultrafast interference imaging of air in splashing dynamics, *Phys. Rev. Lett.*, **107** (15), 154502.

DUCHEMIN, L. & JOSSERAND, C. (2011) Curvature singularity and film-skating during drop impact, *Phys. Fluids*, **23** (9), 091701.

HICKS, P.D. & PURVIS, R. (2010) Air cushioning and bubble entrapment in three-dimensional droplet impacts, *J. Fluid Mech.*, **649**, 135–163.

HOWISON, S.D., OCKENDON, J.R., OLIVER, J.M., PURVIS, R. & SMITH, F.T. (2005) Droplet impact on a thin fluid layer, *J. Fluid Mech.*, **542**, 1–24.

HOWISON, S.D., OCKENDON, J.R. & WILSON, S.K. (1991) Incompressible water-entry problems at small deadrise angles, *J. Fluid Mech.*, **222**, 215–230.

JEFFERY, G.B. (1912) On a form of the solution of Laplace's equation suitable for problems relating to two spheres, *Proc. Roy. Soc. A*, **87** (593), 109–120.

KOLINSKI, J.M., RUBINSTEIN, S.M., MANDRE, S. BRENNER, M.P., WEITZ, D.A. & MAHADEVAN, L. (2012) Skating on a film of air: Drops impacting on a surface, *Phys. Rev. Lett.*, **108** (7), 074503.

KOROBKIN, A.A. (1988) Inclined entry of a blunt profile into an ideal fluid, *Fluid Dyn.*, **23** (3), 443–447.

MANDRE, S. & BRENNER, M.P. (2012) The mechanism of a splash on a dry solid surface, *J. Fluid Mech.*, **690**, 148–172.

MOORE, M.R., HOWISON, S.D, OCKENDON, J.R. & OLIVER, J.M. (2012) A note on oblique water-entry, *J. Engg. Math.*, (in press).

OLIVER, J.M. (2007) Second-order Wagner theory for two-dimensional water-entry problems at small deadrise angles, *J. Fluid Mech.* **572**, 59–85.

PURVIS, R. & SMITH, F.T. (2004) Air-water interactions near droplet impact, *Eur. J. Appl. Math.,* **15** (6), 853–871.

SMITH, F.T., LI, L. & WU, G.X. (2003) Air cushioning with a lubrication/inviscid balance, *J. Fluid Mech.,* **482**, 291–318.

VANDEN-BROECK. J.-M. & SMITH, F.T. (2008) Surface tension effects on interaction between two fluids near a wall, *Quart. J. Mech. App. Math.,* **61** (2), 117–128.

WAGNER, H. (1932) Über Stoß- und Gleitvorgänge an der Oberfläche von Flüssigkeiten, *Z. angew. Math. Mech.,* **12**, 193–215.

XU, L., ZHANG, W.W. & NAGEL, S.R. (2005) Drop splashing on a dry smooth surface, *Phys. Rev. Lett.,* **94** (18), 184505.

RECENT REPORTS

12/81	Inner product computation for sparse iterative solvers on distributed supercomputer	Zhu Gu Liu
12/82	A new pathway for the re-equilibration of micellar surfactant solutions	Griffiths Breward Colegate Dellar Howell Bain
12/83	Object-Oriented Paradigms for Modelling Vascular Tumour Growth: a Case Study	Connor Cooper Byrne Maini McKeever
12/84	Chaste: an open source C++ library for computational physiology and biology	Mirams Arthurs Bernabeu Bordas Cooper Corrias Davit Dunn Fletcher Harvey Marsh Osborne Pathmanathan Pitt-Francis Southern Zemzemi Gavaghan
12/85	A two-pressure model for slightly compressible single phase flow in bi-structured porous media	Schlackow Marguerat Proudfoot Bähler Erban Gullerova
12/86	Boolean modelling reveals new regulatory connections between transcription factors orchestrating the development of the ventral spinal cord	Lovrics Gao Juhász Bock Byrne Dinnyés Kovács
12/87	Asymptotic solutions of glass temperature profiles during steady optical fibre drawing	Taroni Breward Cummings Griffiths
12/88	The kinetics of surfactant desorption at the airsolution interface	Morgan Breward

12/95	On-Lattice Agent-based Simulation of Populations of Cells within the Open-Source Chaste Framework	Figueredo Joshi Osborne Byrne Owen
12/96	Mathematical Biomedicine and Modeling Avascular Tumor Growth	Byrne
12/97	Inference of the genetic network regulating lateral root initiation in Arabidopsis thaliana	Muraro Voß Wilson Bennett Byrne De Smet Hodgman King
12/98	Axisymmetric bifurcations of thick spherical shells under inflation and compression	deBotton Bustamante Dorfmann
12/99	Calculus from the past: Multiple Delay Systems arising in Cancer Cell Modelling	Wake Byrne
12/100	Nonlocal models of electrical propagation in cardiac tissue: electrotonic effects and the modulated dispersion of repolarization	Bueno-Orovio Kay Grau Rodriguez Burrage
12/101	Microfluidic Immunomagnetic Multi-Target Sorting A Model for Controlling Deflection of Paramagnetic Beads	Tsai Griffiths Stone
12/102	A New Lattice Boltzmann Equation to Simulate Density-Driven Convection of Carbon Dioxide	Allen Reis Sun
12/103	Control and optimization of solute transport in a porous tube	Griffiths Howell Shipley

Copies of these, and any other OCCAM reports can be obtained from:

Oxford Centre for Collaborative Applied Mathematics
Mathematical Institute
24 - 29 St Giles'
Oxford
OX1 3LB

England
www.maths.ox.ac.uk/occam